Geological Society, London, Special Publications

Using detrital garnet compositions to determine provenance: a new compositional database and procedure

Simon M. Suggate and Robert Hall

Geological Society, London, Special Publications 2014, v.386;
p373-393.
doi: 10.1144/SP386.8

Notes

Using detrital garnet compositions to determine provenance: a new compositional database and procedure

SIMON M. SUGGATE* & ROBERT HALL

SE Asia Research Group, Department of Earth Sciences, Royal Holloway University of London, Egham, Surrey TW20 0EX, UK

**Corresponding author (e-mail: s.suggate@es.rhul.ac.uk)*

Abstract: Detrital garnet compositions can be used to help determine the provenance of sedimentary rocks. In this study a garnet compositional database consisting of more than 2500 wet chemical and electron microprobe analyses was compiled from the literature. For the garnets in the database the six principal garnet end-member compositions (pyrope, almandine, spessartine, uvarovite, grossular and andradite) were calculated. A multi-stage methodology was devised to match garnet compositions to source rocks, and a series of garnet provenance fields on ternary plots were identified. The method was tested using compositional data from detrital garnet studies in several areas where provenance has already been identified, with good results. The methodology was then used to assess the provenance of detrital garnets from Neogene sandstones of northern Sabah, Borneo for which provenance is unknown and in a region where there are few garnet analyses for comparison. Comparison of garnet compositions from possible sources on Palawan, Philippines and in Borneo combined with the ternary plots excludes some known garnet-bearing rocks as potential sources and suggests derivation of metamorphic and igneous garnets from Palawan during the Early Miocene.

Supplementary material: The compositional database and garnet data plotting spreadsheets are available at www.geolsoc.org.uk/SUP18649

Naturally occurring garnet is potentially a useful provenance indicator. It has a wide compositional variation that may be specific to certain lithologies and, therefore, source areas, it is mechanically resistant during transport, and it is resistant to chemical modification during transport, diagenesis and low-grade metamorphism (e.g. Mange & Morton 2007). Garnets are particularly common in metamorphic rocks, but are also found in acid volcanic rocks, granites and pegmatites, peridotites and kimberlites, and are widespread as detrital grains in sediments.

Chemical analyses of garnets are often expressed as percentages of real or hypothetical molecules – the ‘garnet end-members’ (Deer *et al.* 1962, 1966, 1997; Rickwood 1968). The end-member molecules provide a qualitative summary of garnet composition that is useful in provenance studies as the data can be displayed on ternary plots so that comparisons between sediment and potential sources can be made. Garnets have been used as a provenance indicator in a number of studies (Morton 1985; Haughton & Farrow 1989; Tebbens *et al.* 1995; Hutchison & Oliver 1998; Oliver 2001; Sabeen *et al.* 2002; Morton *et al.* 2004; Copjakova *et al.* 2005; Win *et al.* 2007; Hallsworth & Chisholm 2008). Many of these studies have successfully matched garnets to local sources. However, the range of garnet compositions is very wide, and it is not known if all garnets can be matched to source rocks. Furthermore, in regions where the sources are unknown, or have been removed by erosion, or where there are no compositional data from garnet-bearing rocks, it is not clear if compositional data from other regions of the world can be reliably used to infer protoliths and provenance. This paper discusses a large garnet compositional database compiled from the literature which was used to examine how useful such data could be in identifying the provenance of detrital garnets. We find that although not all garnets can be matched uniquely to particular source rocks, many garnets are useful for provenance interpretation. It is necessary to calculate the common garnet end-members (almandine, andradite/schorlomite, grossular, pyrope, spessartine and uvarovite), then follow a series of steps before plotting compositions on ternary diagrams. The new procedure has been applied successfully to determine the provenance of detrital garnets from Neogene sandstones of northern Borneo.

Garnet mineralogy

The garnet group can be considered as a number of common molecules (Table 1) which represent the

From: Scott, R. A., Smyth, H. R., Morton, A. C. & Richardson, N. (eds) 2014. *Sediment Provenance Studies in Hydrocarbon Exploration and Production*. Geological Society, London, Special Publications, **386**, 373–393.
First published online July 18, 2013, http://dx.doi.org/10.1144/SP386.8

Table 1. *Garnet end-members of the isomorphous series*

	Specific gravity (D)	
Pyrope	3.58	$Mg_3Al_2Si_3O_{12}$
Almandine	4.32	$Fe_3Al_2Si_3O_{12}$
Spessartine	4.19	$Mn_3Al_2Si_3O_{12}$
Uvarovite	3.90	$Ca_3Cr_2Si_3O_{12}$
Grossular	3.59	$Ca_3Al_2Si_3O_{12}$
Andradite	3.86	$Ca_3Fe_2Si_3O_{12}$

end-members of isomorphous series (Deer *et al.* 1962, 1997). These species form two solid solution series: the Pyralspite group (pyrope, almandine and spessartine) and Ugrandite group (uvarovite, grossular, and andradite). It is unusual for any garnet to be a pure end-member composition, and most garnets are solid solutions of several end-members. The summary of garnet mineralogy and paragenesis below is based on Deer *et al.* (1962, 1966, 1997).

Pyralspite group

There are three end-members for the Pyralspite garnets: pyrope, almandine and spessartine.

Pyrope. $Mg_3Al_2Si_3O_{12}$-rich garnets occur in certain ultrabasic rocks, including peridotites, kimberlites and xenocrysts in basalt pipes.

Almandine. $Fe_3Al_2Si_3O_{12}$-rich garnets are typical of garnetiferous schists resulting from the regional metamorphism of argillaceous sediments and basic igneous rocks. Almandine also occurs in some thermal or contact aureoles, in contaminated granites, and as xenocrysts in some volcanic rocks. The garnet in granulite facies rocks is commonly almandine or more rarely almandine–pyrope. In eclogite facies rocks the garnet is typically almandine–pyrope, often with almandine percentages greater than pyrope percentages.

Spessartine. $Mn_3Al_2Si_3O_{12}$-rich garnets are commonly found in granites, granitic pegmatites, often as spessartine–almandine. Spessartine also occurs in some skarn deposits, in Mn-rich assemblages of metasomatic origin, within veins in metamorphosed greywackes, and is also known from Mn-rich cherts in blueschist facies rocks.

Ugrandite group

There are three end-members for Ugrandite garnets: uvarovite, grossular and andradite.

Uvarovite. $Ca_3Cr_2Si_3O_{12}$-rich garnets are the least common of the anhydrous garnet species. Garnets with uvarovite as the dominant molecule are found mainly in serpentinites and chlorite schists, often in association with chromite, and in metamorphosed limestones and skarn ore-bodies.

Grossular. $Ca_3Al_2Si_3O_{12}$-rich garnet is characteristic of thermally and regionally metamorphosed impure calcareous rocks. Hydrogrossular garnets are found in metamorphosed marls and are common in rodingites and altered rocks associated with serpentinites.

Andradite. $Ca_3Fe_2Si_3O_{12}$-rich garnet commonly occurs in contact or thermally metamorphosed impure calcareous sediments, as well as in metasomatic skarn deposits that are often associated with thermal metamorphism. Deer *et al.* (1962) considered melanite and schorlomite as Ti-bearing varieties of andradite but Rickwood (1968) suggested that *schorlomite* ($Ca_3Ti_2Fe_2TiO_{12}$) should be considered a separate molecule. The Ti-rich andradite garnets are found mainly in alkaline igneous rocks and skarns.

Garnet end-members

Chemical analyses of garnets are often expressed as percentages of real or hypothetical molecules of extreme composition – the 'garnet end-member' molecules (Deer *et al.* 1962, 1997; Rickwood 1968). The end-member molecules provide a qualitative summary of garnet composition, as the data can be plotted quickly on ternary plots. As outlined above, Deer *et al.* (1962) considered six important end-members. Since then a number of authors (Rickwood 1968; Knowles 1987; Muhling & Griffin 1991; Locock 2008) have suggested that additional end-members should be considered. Deer *et al.* (1997) included several other end-members in their compilations of garnet compositions in addition to the six main species. Rickwood (1968) identified 19 end-members and Locock (2008) calculated 29. They developed procedures using stand-alone computer programs or spreadsheets to allow users to calculate the molecular proportions of garnet end-members from chemical analyses. The procedure suggested by Locock (2008) uses an Excel spreadsheet to calculate 29 end-members (15 naturally occurring and 14 hypothetical end-members) for each analysis. However, this procedure is not very useful in provenance studies because 14 of the end-members calculated are not naturally occurring and cannot be assigned to a protolith for provenance interpretations, and of the 15 naturally occurring garnets, a number are unusually rich in elements that are exceptionally rare in most geological environments and, in fact, have mainly not been reported from detrital garnets (Mange & Morton 2007). The large number of end-members make the data difficult to display on diagrams and, because of these limitations, a new approach has been devised.

We found that because of the rarity of extreme compositions it is sufficient to screen the data to identify those that are unusual, for example, in having high contents of Zr, Y, V and Ti. If such garnets were to be found in detrital assemblages they could be matched to source rocks very easily. We then identified a series of steps, described below, for examining the data, and finally the end-member compositions are plotted on ternary diagrams.

We used Pascal computer programs to input the data and to calculate garnet formulae on the basis of 24 oxygens in order to estimate ferric iron, and then calculated the common garnet end-member compositions: pyrope, almandine, spessartine, uvarovite, grossular and andradite. Schorlomite was combined with andradite for garnets with less than 2 wt% TiO_2. The programs are available from the authors on request. We compared the results of the calculations with garnet end-members listed by Deer *et al.* (1966) and Locock (2008). Molecular percentages of end-member components for six typical garnets (Table 2) of various compositions were recalculated from the oxide weight percentages listed by Deer *et al.* (1966) using the Locock (2008) method and the method of this study, and were compared with end-members given by Deer *et al.* (1966). The results (Table 3) are in good agreement.

Garnet compositional database

The garnet compositional database (Supplementary material) consists of more than 2500 wet chemical and electron microprobe analyses that were compiled from more than 150 published data sources. Data are listed in a single table containing oxide wt% compositions (SiO_2, TiO_2, Al_2O_3, Cr_2O_3, Fe_2O_3, FeO, MnO, MgO, CaO, Na_2O and rare oxides V_2O_3, Y_2O_3, ZrO_2 if present) and calculated end-member compositions, together with the published garnet source rock/protolith, grade, pressure, temperature and the literature source. A number of ternary plots of garnet compositions from the database are presented in an Excel spreadsheet (Supplementary material).

It can be problematic to determine provenance of detrital garnets using plots in which end-member compositions are combined (e.g. almandine + spessartine, grossular + andradite + uvarovite) in order to produce a single ternary diagram. An example of this is shown in Figure 1. The ternary plot shows that when end-member compositions are combined it may be very difficult to identify specific protoliths, as many of the data points plot as clusters in similar or overlapping areas. Different authors have chosen different ways in which to combine garnet end-members, commonly so that they can use just one triangle to display garnet compositions. We found a single triangle was too restrictive and often caused overlap of otherwise distinctive protoliths. We tried several different combinations and found that two triangular plots were most effective in discriminating between different protolith compositions and metamorphic grades. The apices of the triangles are almandine, pyrope, spessartine and grossular + andradite + schorlomite.

Using the database a multi-stage methodology was devised which identifies the protoliths and/or metamorphic grade of garnets therein. Stage 1 removed garnets with unusual contents of Y_2O_3,V_2O_3 and ZrO_2. Stage 2 excluded garnets with unusually high contents of TiO_2. The garnets identified in Stages 1 and 2 can be matched to unusual protoliths (e.g. ores, skarns, mafic pyroclastic rocks and nepheline syenites). After the unusual garnet compositions were excluded the next stages matched the remaining garnet compositions to specific protoliths and/or metamorphic grade. Stages 3–5 identified garnets with high uvarovite and pyrope contents which are mostly typical of

Table 2. *Analyses of garnets from Deer* et al. *(1966)*

		SiO_2	TiO_2	Al_2O_3	Cr_2O_3	Fe_2O_3	FeO	MnO	MgO	CaO
Quartz–biotite gneiss	DHZ 1	38.03	0.00	22.05	0.00	0.88	29.17	1.57	6.49	1.80
Metamorphosed andesite	DHZ 2	37.03	0.04	8.92	0.00	18.34	2.25	1.09	0.83	30.26
Anorthite–clinozoisite–corundum–garnet gneiss	DHZ 3	38.69	0.55	18.17	0.00	5.70	3.78	0.64	0.76	31.76
Eclogite	DHZ 4	41.52	0.01	23.01	0.22	1.22	12.86	0.33	16.64	4.71
Calcsilicate hornfels	DHZ 5	35.84	0.03	20.83	0.00	0.65	1.78	33.37	2.48	5.00
Uvarovite–tremolite–tawmawite–pyrrhotite rock	DHZ 6	35.88	0.00	1.13	27.04	2.46	0.00	0.03	0.04	33.31

Table 3. *Comparison of molecular percent end-members calculated for garnet compositions of Table 2 by Deer* et al. *(1966), Locock (2008) and this study*

	This study						Deer *et al.* (1966)						Locock (2008)					
	DHZ 1	DHZ 2	DHZ 3	DHZ 4	DHZ 5	DHZ 6	DHZ 1	DHZ 2	DHZ 3	DHZ 4	DHZ 5	DHZ 6	DHZ 1	DHZ 2	DHZ 3	DHZ 4	DHZ 5	DHZ 6
Almandine	63.7	6.7	8.7	26.2	–	0.3	65.4	5.2	8.1	26.1	4.0	–	63.8	5.1	8.1	25.9	0.2	–
Andradite + Schorlomite	–	58.9	16.2	–	7.6	8.2	2.7	56.9	18.2	3.3	2.2	7.7	–	56.4	16.6	–	2.0	5.6
Grossular	5.4	28.6	70.9	11.7	6.8	1.9	2.5	32.0	69.4	8.9	11.2	2.4	5.0	32.0	69.5	11.5	6.6	4.5
Pyrope	27.2	3.3	2.9	60.7	9.9	0.2	25.8	3.4	2.9	60.3	7.9	0.2	25.3	3.4	2.9	59.8	9.9	0.2
Spessartine	3.7	2.5	1.4	0.7	75.7	0.1	3.6	2.5	1.4	0.7	74.7	0.1	3.5	2.5	1.4	0.7	75.6	0.1
Uvarovite	–	–	–	0.6	–	89.4	–	–		0.7	–	89.6	–	–	–	0.6	–	88.9
Total	100.0	100.0	100.1	99.9	100.0	100.1	100.0	100.0	100.0	100.0	100.0	100.0	97.6	99.4	98.4	98.6	94.2	99.2

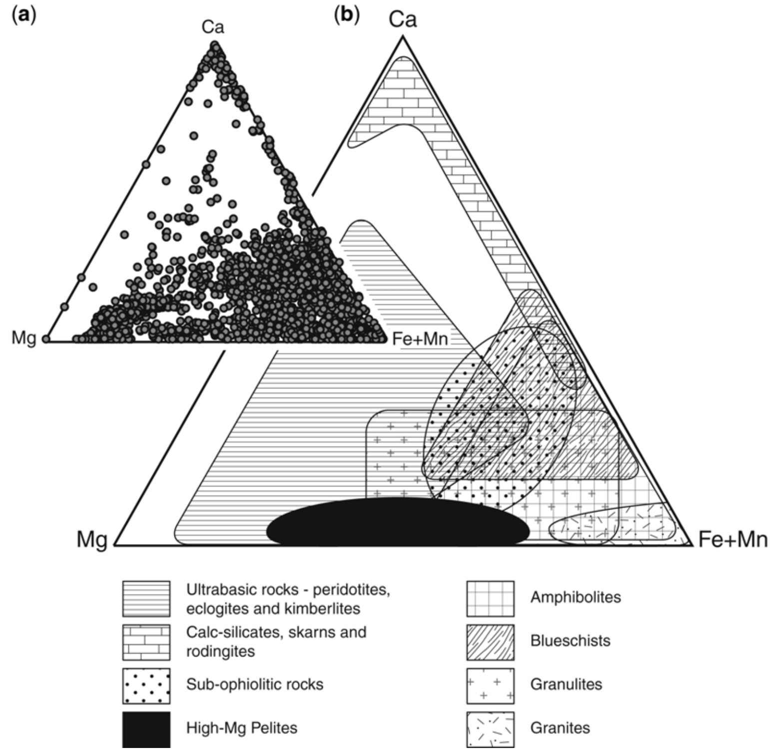

Fig. 1. Ternary plots showing all garnet data. (**a**) All garnets from the database ($n = 2400$) excluding those with unusual rare oxide contents (V_2O_3, Y_2O_3, ZrO_2) and $TiO_2 > 2$ wt%, as discussed in the text. (**b**) All garnet compositions grouped by protolith. Ca, Mg, Fe and Mn are ionic contents of those elements calculated on the basis of 24 oxygens normalized to total $Ca + Mg + Fe^2 + Mn$. When end-member compositions are combined in a single ternary plot it is difficult to distinguish many protoliths because of overlaps of compositional areas for different types.

ultrabasic protoliths. Then different groups of garnets were plotted on the ternary diagrams to establish the compositional areas. The sequence and rationale is summarized below. Observations made from each stage are also detailed below. The areas for garnets from different protoliths and different metamorphic grades are plotted on a series of ternary plots in Figures 2 and 3.

Stage 1: high rare oxide contents

This stage identified all garnets with extreme Y_2O_3, V_2O_3 and ZrO_2 contents and removed them from the database. There is a very small number of such garnets. Y-rich garnets ($n = 24$) range up to 3.4 wt% Y_2O_3. They are found in Y-rich gneisses, granite pegmatites and one hornfels. V-rich garnets ($n = 24$) range from 0.02 to 22.1 wt% V_2O_3. The V-rich garnets are found mainly in metaironstones, a few metasediments, unusual mafic pyroclastic rocks and ore deposits. Several of the V-rich garnets also have high Cr contents. There are only nine Zr-rich garnets (up to 29.9 wt% ZrO_2) which are from a skarn/rodingites, a carbonatite and a calc-silicate. It is also notable that such unusual garnets are commonly enriched in more than one rare oxide; for example, scandium-rich garnets from Russia (Galuskina *et al.* 2005) are also rich in Hf, Y, V and Zr. It is unusual for any of these elements to be reported, which probably implies unusual compositions or environments of garnet formation when they are determined. We arbitrarily excluded all garnets that have greater than 0.1 wt% of these oxides. In detrital studies this value could probably be set higher, for example, at 1 wt%, since garnet compositions are typically determined for garnet cores, and the lower values in our dataset are commonly rims to garnet with cores that have larger enrichments than 1 wt%.

Stage 2: high TiO_2 contents

This stage identified all garnets with high TiO_2 contents, and we chose an arbitrary cut-off value

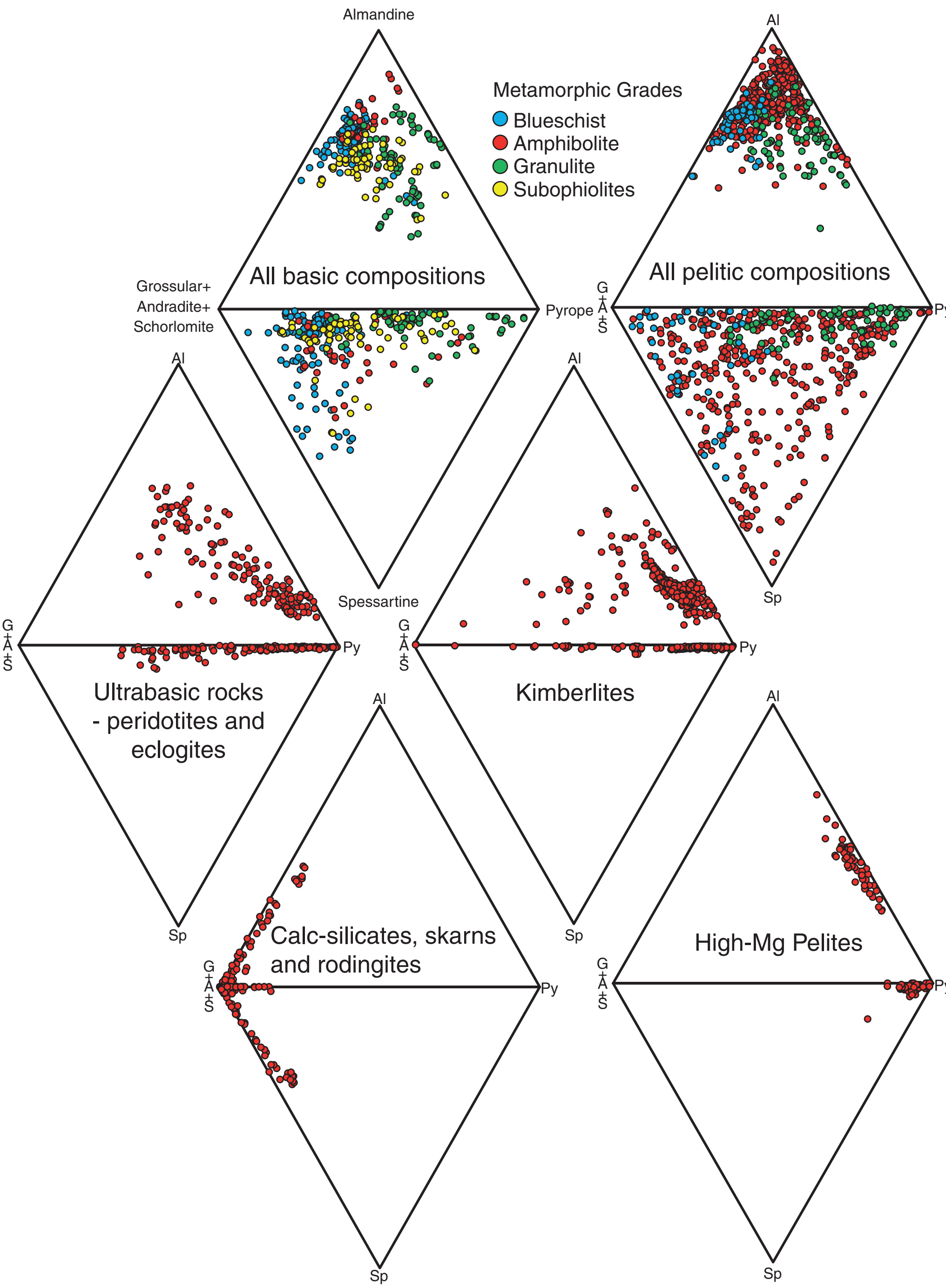

Fig. 2. Ternary plots using end-members grossular + andradite + schorlomite, almandine, pyrope and spessartine for various protolith compositions. Garnets were selected for different protoliths after excluding those with unusual rare oxide contents (V_2O_3, Y_2O_3, ZrO_2) and TiO_2 >2 wt% as discussed in the text.

of 2%, which excluded a relatively small number ($n = 44$) of garnets with up to 19.6 wt% TiO_2. Garnets excluded at this stage are almost all skarns and nepheline syenites, with a few unusual calc-silicates.

Stage 3: high pyrope and high uvarovite contents

This stage identified garnets with pyrope contents >55% and uvarovite contents >1%. Based on trial and error we found that these values identified only garnets with ultrabasic protoliths, including various peridotites, kimberlites and some eclogites (types A and B of Coleman *et al.* 1965). Because these garnets all have very low spessartine contents they plot on the almandine, pyrope, grossular + andradite + schorlomite triangle in the area with pyrope >55%.

Stage 4: high uvarovite contents

This stage identified all remaining garnets with high uvarovite content. There is a very small number of garnets ($n = 29$) that have uvarovite >1% and do not have pyrope contents >55%. These are mainly from ultrabasic rocks, ores, skarns or kimberlites.

Stage 5: high pyrope contents

This stage identified all remaining garnets with high pyrope contents. There is a small number ($n = 118$) of garnets that have pyrope contents >55% and do not have uvarovite >1%. The majority of these have ultrabasic protoliths, mainly various peridotites and kimberlites. The remainder consists mainly of Mg-rich granulites. Thus after stage 3, garnets from ultrabasic rocks can be identified with confidence and, if the uvarovite content is ignored, 95% of the garnets that plot on the almandine, pyrope, grossular + andradite + schorlomite triangle in the area with pyrope >55% can be identified as having an ultrabasic protolith. Most of the remaining garnets that fall in this area are unusual high-Mg pelites of granulite facies grade.

Stage 6: remaining garnets

After a number of trials testing various criteria for selecting values we found that simply plotting garnet compositions on the two triangles with apices of almandine, pyrope, spessartine and grossular + andradite + schorlomite was an effective way to identify garnet from many rock compositions, or that correspond to different metamorphic grades. Figure 4 shows the sub-areas characteristic of garnets with different protoliths. The sub-areas we have identified are similar to those identified by Mange & Morton (2007) which they named as garnet types A, Bi, Bii, Ci and Cii. Hutchison & Oliver (1998) and Oliver (2001) used similar end-members. We were not able to replot on our triangles the garnets they used, as their data are not available, but we did plot our data on their X_{Mg}–X_{Ca}–X_{Fe+Mn} triangle. This broadly confirmed that different protoliths can be identified using their single or our double triangle. However, we consider that a better separation of some garnet types can be made using the two triangles rather than the single X_{Mg}–X_{Ca}–X_{Fe+Mn} triangle they used. Furthermore, some garnet types are missing or not shown on the earlier plots. For example, Mange & Morton (2007) have no blueschist or sub-ophiolite garnets, while Hutchison & Oliver (1998) and Oliver (2001) used only part of the triangle, so excluding many calc-silicate and ultrabasic garnets. In addition, we now have a much larger database of garnet compositions. This means that some fields are larger than those identified by Hutchison & Oliver (1998) and Oliver (2001); for example, their granulite field included a small number of Lewisian garnets, whereas we now have many more garnets from granulite rocks world-wide. Their plots were effective because it was certain that garnets had a Scottish source but their compositional areas may not be so useful when comparing garnets from other parts of the world. The larger database with more protolith types gives more confidence that garnets can be matched to sources, noting that it will still be valuable to continue enlarging the database, which we intend to do. We summarize below the main features of the database garnets and the ternary plots.

Protolith compositions

Figure 4 shows the main sub-areas that we have identified using the methods explained above. Most garnets from ultrabasic rocks–peridotites, eclogites and kimberlites–can be identified by their pyrope contents >55% (Fig. 4a). Skarns and calc-silicates can also be identified confidently by their high grossular(+andradite + schorlomite) and very low pyrope contents. Granites (which include large intrusive bodies, leucosomes and migmatites) typically have very high almandine contents and can usually be distinguished from other almandine-rich garnets by their high spessartine contents. Blueschist, amphibolite, granulite facies and sub-ophiolite garnets overlap (Fig. 4b, c), but can often be separated, as explained below. Many basic eclogite garnets plot in the same areas, but can usually be distinguished by their very low spessartine contents.

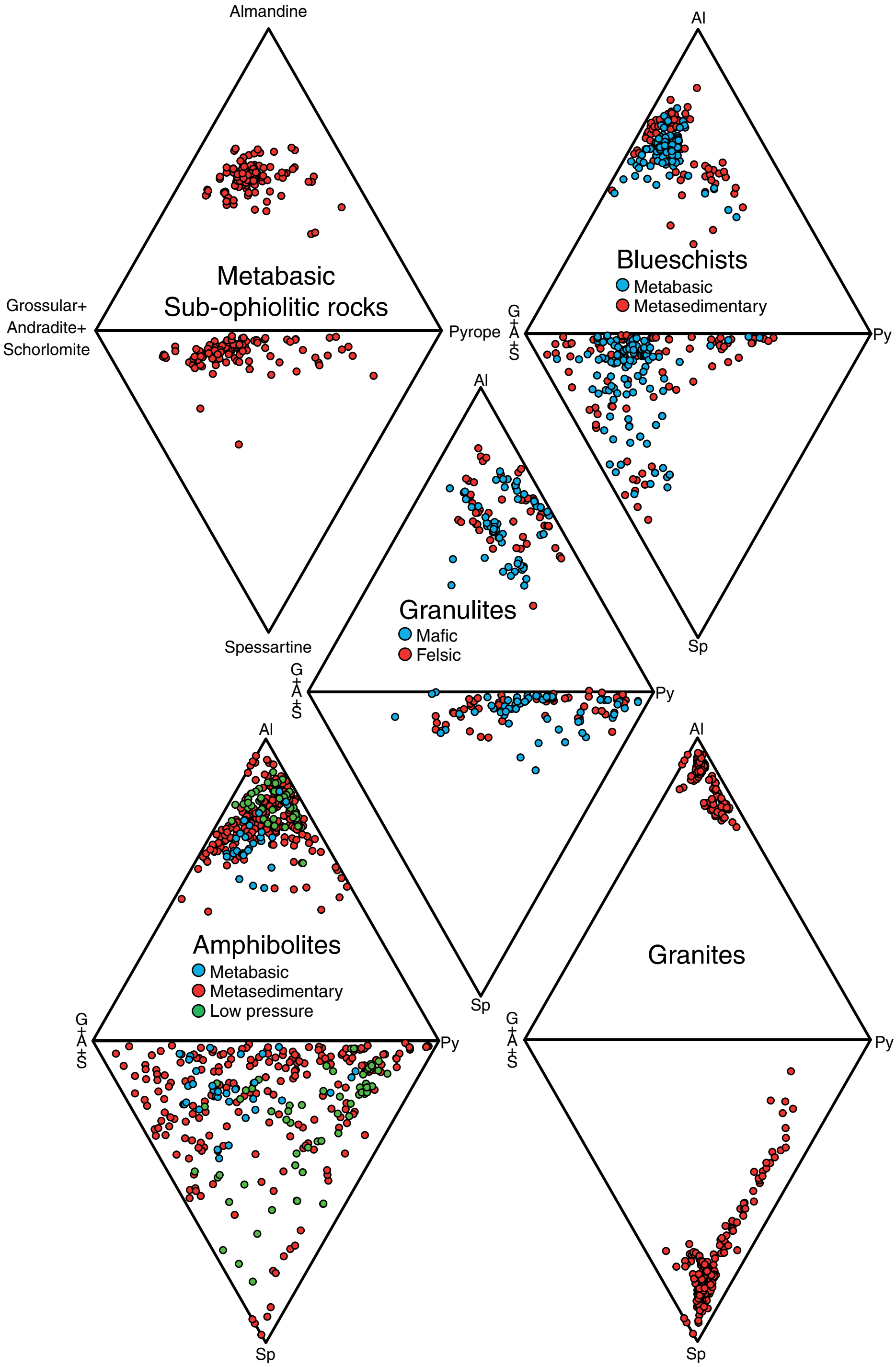

Fig. 3. Ternary plots using end-members grossular + andradite + schorlomite, almandine, pyrope and spessartine for protolith compositions and different metamorphic grades, and granites. Granites include large intrusive bodies, leucosomes and migmatites. Garnets were selected for the different categories after excluding those with unusual rare oxide contents (V_2O_3, Y_2O_3, ZrO_2) and TiO_2 >2 wt%, as discussed in the text.

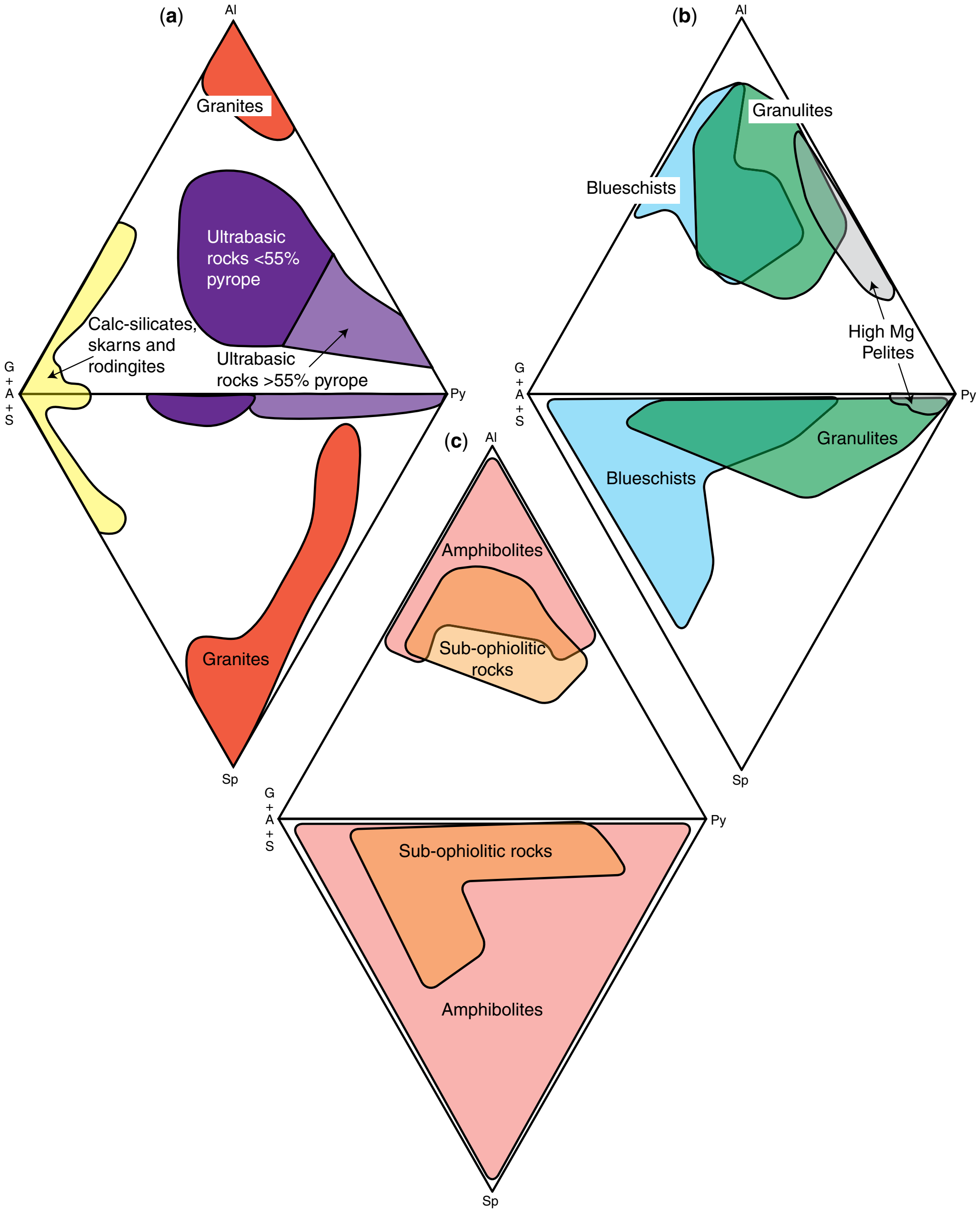

Fig. 4. Ternary plots using end-members grossular + andradite + schorlomite, almandine, pyrope and spessartine showing sub-areas characteristic of garnets with different protoliths. (**a**) Ultrabasic rocks (peridotites, eclogites and kimberlites); granites; and calc-silicates, skarns and rodingites. 95% of all ultrabasic garnets have pyrope >55%. (**b**) Granulites, granulite facies high-Mg pelites, and blueschists. (**c**) Amphibolites and metabasic sub-ophiolitic rocks.

Metamorphic grade

After ultrabasic rocks, calc-silicates and granites (Fig. 4a) have been identified, there is a large area where many garnets plot. These garnets are mainly from blueschist, amphibolite and granulite facies rocks and sub-ophiolite metabasites. Figure 4b shows garnets of blueschists and granulite facies rocks from two common rock compositions: pelites and metabasites. Many blueschist and granulite facies garnets can be separated on the triangles, although there is some overlap. Metabasite sub-ophiolite garnets overlap with blueschist, amphibolite and granulite facies garnets (Fig. 4c). Compositions of amphibolite facies garnets from basic rocks are not abundant in the literature, presumably because metabasite mineral assemblages are not very useful in determining PT conditions. In contrast, compositions of pelitic garnets from amphibolite facies rocks are abundant and they tend to be more almandine-rich than either blueschist or granulite garnets. The plots show that, although many of these garnets cannot be matched to protoliths, a reasonable number can be. Pyrope-poor grossular-almandine garnets are likely to be from blueschists (Fig. 4b), and grossular-poor pyrope-almandine garnets are likely to be from granulites (Fig. 4b). Extremely almandine-rich pyrope-grossular-poor garnets are either amphibolite facies garnets from pelites (Fig. 4c) or from granites (Fig. 4a), but granite garnets can usually be identified by their higher spessartine contents.

Application to detrital garnets

The methodology above was developed using the large database to evaluate how useful garnet compositions could be in provenance analysis and to identify specific garnet compositions that could be matched to protoliths. Here we test the method using earlier studies.

The Excel spreadsheet (Supplementary material) that contains the database allows a rapid selection of different garnets based on compositional and metamorphic grade criteria. We first examined the dataset garnets using plots used by authors including Mange & Morton (2007), Win *et al.* (2007) and Méres *et al.* (2012) who have shown that garnets can be subdivided into different protolith types and metamorphic grades. Using the triangles they suggested confirms that garnets from the database do fall into the fields they identified. However, in all cases we found the triangles chosen were too restrictive and resulted in overlaps of some garnet types. As explained above, we found the most effective separation of different garnet types was achieved using triangles with apices of almandine, pyrope, spessartine, and grossular + andradite + schorlomite. The papers of Mange & Morton (2007) and Win *et al.* (2007) do not include their large datasets of garnet analyses so we are unable to replot their garnets on our diagrams for comparison. Because they considered garnets from potential sources in the same region they were able to make quite precise matches to protoliths. Although we cannot identify all their subtypes, we can confirm the main protoliths they identify. We have replotted the dataset of Méres *et al.* (2012), and this is discussed below.

Below we test the method by using a number of recent studies that published chemical analyses of detrital garnets and interpreted their provenance, and we compare the conclusions of the earlier works with our interpretations based on the ternary plots. In each case the earlier works compared garnets to those from protoliths in the studied region (Fig. 5). We then discuss the application of the method to garnets in Borneo sandstones where the provenance is unknown and there are few analyses of garnets from potential source rocks.

Algeria

Kahoui *et al.* (2012) analysed detrital garnets from Pliocene to Quaternary sands and Lower Cretaceous sandstones in the El Kseibat area, where detrital diamonds have also been found. The primary sources of the diamonds and garnets are not known, but sediments containing numerous kimberlite indicator mineral grains such as pyrope garnet, chrome spinel and picroilmenite are known from an area up to 1000 km wide within which is the Djebel Aberraz diamond placer deposit. The compositions of the detrital garnets are plotted in Figure 5a. They fall unambiguously in the area of ultrabasic protoliths found in mantle xenoliths and kimberlites.

Eastern Europe

Aubrecht *et al.* (2009) analysed heavy minerals from Cretaceous marly limestones of the Czorsztyn Unit in the western Carpathians. They interpreted the majority of detrital garnets to be derived from high pressure/ultra-high pressure (HP/UHP) parental rocks which recrystallized under granulite and amphibolite facies conditions, probably originally derived from magmatic and metamorphic rocks of the Oravic basement.

Based on the ternary plots (Fig. 5b1) it is possible to exclude protoliths such as ultrabasic rocks, kimberlites, eclogites and calc-silicates. On the ternary triangles the garnets plot in areas that include basic and pelitic rocks from a wide range of metamorphic conditions including blueschists, amphibolites, granulites and sub-ophiolite soles. Some of the garnets cannot be from blueschists or sub-ophiolite soles. It is possible to say that most of the garnets, notably those which are grossular-poor, could only have come from amphibolite and granulite facies rocks of basic and pelitic

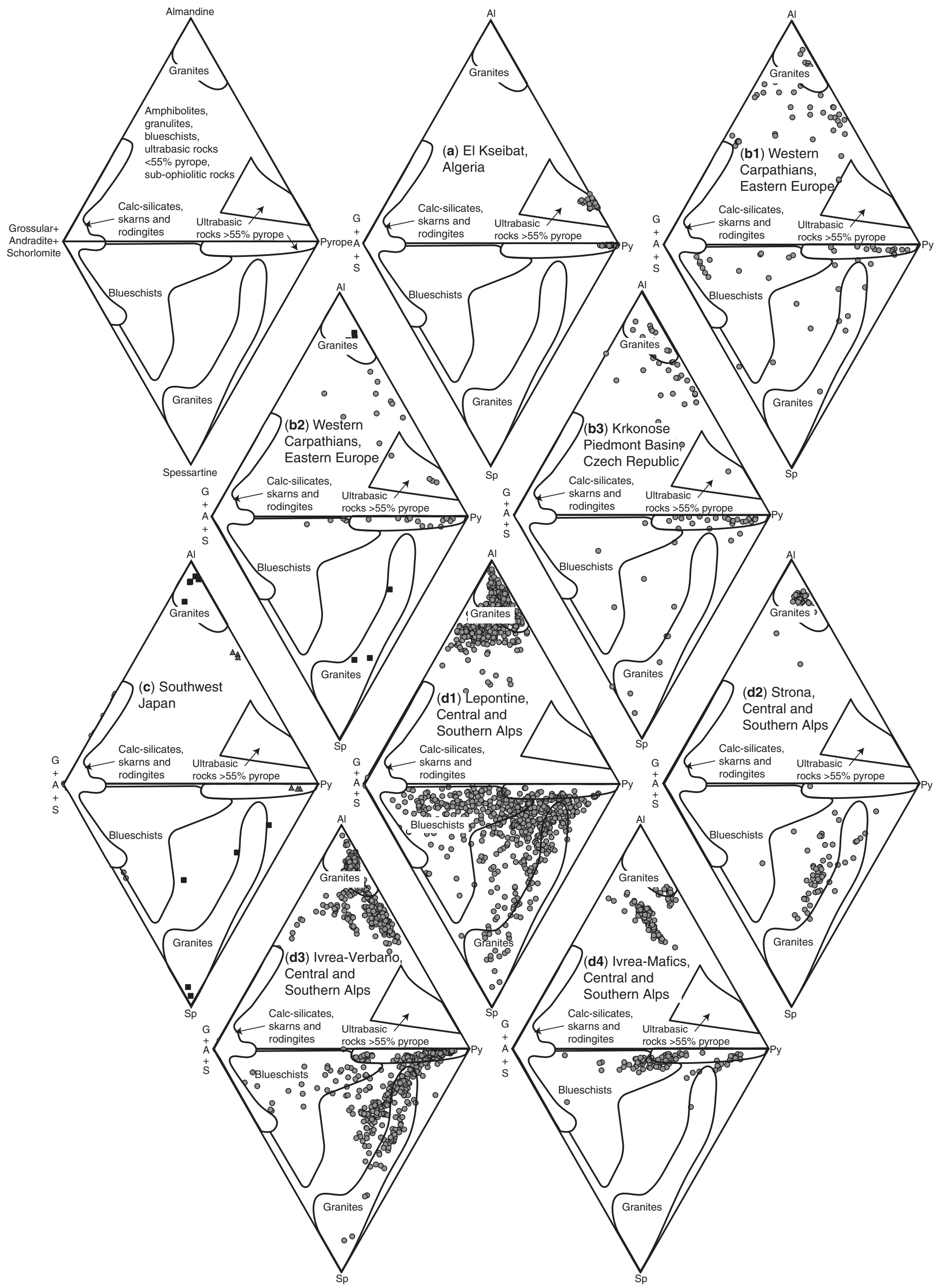

Fig. 5. Detrital garnet compositions from provenance studies in Algeria (Kahoui *et al.* 2012), Western Carpathians, Eastern Europe (Aubrecht *et al.* 2009; Méres *et al.* 2012), Czech Republic (Martínek & Štolfová 2009), Japan (Takeuchi 1994; Takeuchi *et al.* 2008), Central and Southern Alps, Italy–Switzerland (Andò *et al.* 2013).

compositions, and all of the garnet could be from amphibolite facies rocks. A few garnets could have granitic protoliths which were migmatites.

Méres *et al.* (2012) described detrital garnets from Jurassic sandstones which they interpreted to be derived from HP/UHP metamorphic rocks including garnet peridotites, eclogites and granulites. Their conclusions are supported by the presence of kyanite and omphacite inclusions in pyrope-rich garnets. The ternary plots (Fig. 5b2) show it is possible to exclude calc-silicate and blueschist facies protoliths, and they are unlikely to have amphibolite facies protoliths of any composition. A small number of the garnets have granitic protoliths. Some definitely have ultrabasic protoliths. The low spessartine contents of the majority most closely resemble garnets from granulites and deep crustal eclogites.

Martínek & Štolfová (2009) reported heavy mineral assemblages and garnet compositions from Permian terrestrial sediments of the Krkonoše Piedmont Basin in the Czech Republic. They interpreted detrital garnet compositions to indicate sources to include Moldanubian granulites, garnet clinopyroxenites, leucogranites and pegmatites. The ternary plots (Fig. 5b3) show that some garnets probably have granitic protoliths. One definitely has an ultrabasic protolith. Calc-silicate and blueschist facies protoliths can be ruled out. The majority most closely resembles garnets from granulite facies rocks, but amphibolite facies rocks cannot be excluded.

Japan

Takeuchi (1994) and Takeuchi *et al.* (2008) reported analyses of detrital garnets from Permian–Jurassic sandstones of two different terranes in SW Japan. Although many garnets were analysed in each study only 10 analyses are reported in each paper so the two subsets have been combined here. The garnet compositions are quite different from those from Algeria and East Europe. They were interpreted to be derived from intrusive rocks, low-grade or contact rocks such as skarns or hornfels, and high grade metamorphic rocks including granulites. The ternary plots (Fig. 5c) show that blueschist facies and ultrabasic protoliths can be excluded. The majority of garnets in the two areas have calc-silicate protoliths. Several have granite protoliths. The remaining garnets most closely resemble garnets from granulite facies rocks.

Central and southern Alps, Italy–Switzerland

Andò *et al.* (2013) compiled a very large number of detrital garnet analyses as part of a heavy mineral study of river sands derived from source rocks of high-grade metamorphic rocks in a section across the Central and Southern Alps, including the Cenozoic amphibolite facies core of the Lepontine Dome and Palaeozoic granulite facies rocks of the Ivrea–Verbano Zone. They were able to match the detrital garnet compositions to local source rocks and showed that they included amphibolite facies low-Mg garnets, high-Mn garnets from granite pegmatites, almandine–pyrope-rich garnets from granulite facies metasediments and almandine–pyrope–grossular garnets from metagabbros. They suggested an ultrabasic protolith for a few Lepontine garnets.

The ternary plots (Fig. 5d1–4) show garnets from the four sub-areas. The plots support the conclusions of Andò *et al.* (2013) and show that even in the absence of information about source rocks and garnet compositions, the garnets can provide valuable information about protoliths. Blueschist facies rocks can be ruled out for the Strona area (Fig. 5d2) and the Ivrea mafic rocks (Fig. 5d4), and probably for the Ivrea–Verbano area (Fig. 5d3). Blueschist facies rocks cannot be ruled out for some of the Lepontine garnets (Fig. 5d1), but most cannot be from blueschist facies protoliths and are typical of amphibolite facies rocks and granites (probably migmatites). There may be rare calc-silicate garnets in the Lepontine and Ivrea–Verbano areas, but not in the Strona or Ivrea Mafic areas. The majority of Strona garnets have a granitic protolith. The majority of Ivrea–Verbano garnets are likely to be from granulite facies rocks but the most almandine-rich garnets do not resemble granulites and can be matched in our database either by amphibolite facies or granitic garnets. The Ivrea Mafic area garnets are from granulite facies rocks. We differ only from Andò *et al.* (2013) in the suggestion of ultrabasic garnets. None of the alpine garnets resembles those with ultrabasic protoliths in our database, and they are all much less Mg-rich than those reported from potential Alpine peridotite sources (e.g. Evans & Trommsdorff 1978; Nimis & Trommsdorff 2001).

Northern Sabah, Borneo

Neogene sandstones from northern Borneo contain varying amounts of garnet. There are a number of possible source areas for these garnets in Borneo itself, but there are no analyses of garnets from any of these areas. Heavy mineral studies (van Hattum 2005; Suggate 2011; van Hattum *et al.* 2013) suggested that the sandstones could have a Philippines source, and there are a small number of analyses of garnets from potential source rocks in Palawan.

Sabah geology and stratigraphy

The sedimentary rocks of Sabah, northern Borneo (Fig. 6) were deposited in two distinctly different phases. The first phase predates the Top Crocker Unconformity (TCU) of Early Miocene age (van Hattum *et al.* 2006), and is characterized by deep-marine sedimentation. These sedimentary rocks include the Upper Cretaceous to Eocene Sapulut Formation (Rajang Group) and Eocene to Lower Miocene Trusmadi and Crocker formations (Crocker Group). The second phase of sedimentation post-dates the TCU and occurred after arc–continent collision in the Early Miocene uplifted and deformed the strata of the Rajang Group and Crocker Group. Subsidence resumed and sedimentation continued in a fluvio-deltaic to shallow-marine setting, depositing the thick sequences of Neogene clastic sediments in northern and central–eastern Sabah. In northern Sabah (Fig. 6), the Neogene rocks comprise the Lower to Middle Miocene Kudat Group which consists of the Lower to Middle Miocene Kudat Formation and the Upper Miocene Bongaya Formation.

The Kudat Formation (Fig. 6) is divided into the clastic Tajau Sandstone Member and Sikuati Member, which are overlain by a series of mudstone and limestone members (Stephens 1956). The Kudat Formation is composed of interbedded shallow-marine sandstones and mudstones. The Tajau Sandstone Member consists predominantly of gently folded thick coarse sandy proximal debris flows. The Sikuati Member sits stratigraphically above the Tajau Sandstone Member and consists of well-laminated tilted sandstones, siltstones and mudstones, with few sedimentary structures. Biostratigraphical re-evaluation of the foraminiferal assemblages in the Tajau Sandstone Member by BouDagher-Fadel (pers. comm. 2011) confirms initial suggestions by Clement (1958) and van Hattum (2005) that the Eocene foraminifera originally used by Stephens (1956) as age determining are reworked. BouDagher-Fadel (pers. comm. 2011) confirms assemblages present are of Late Oligocene–Early Miocene age, and the presence of *Miogypsinella ubaghsi* indicates a lowermost Early Miocene age of *c.* 21–23 Ma (Early Aquitanian–Early Te5 Letter Stage; BouDagher-Fadel, 2008) for the Tajau Sandstone Member.

Provenance of northern Sabah Lower Miocene sandstones

A provenance study of the Lower Miocene Tajau Sandstone Member of northern Sabah (Suggate 2011) shows that based on light minerals the sandstones are compositionally and texturally immature. The sandstones are predominantly arkoses, feldspathic litharenites and litharenites. Monocrystalline quartz (<60%) and potassium feldspar (*c.* 20–30%) are dominant. Chert is present, although always in small amounts, and is probably derived from the local basement. The heavy mineral assemblage of the Tajau Sandstone Member is dominated by zircon (max. 45% and mean 29%) and garnet (max. 50% and mean 24%). Apatite is present in significant amounts (*c.* 10–15%). The zircons are typically a mixture of euhedral (21%), subhedral (42%) and subrounded (15%) grains. Medium- to high-grade metamorphic minerals present include kyanite, sillimanite, andalusite, epidote and staurolite. This is in marked contrast to the overlying Sikuati Member, in which heavy mineral assemblages are dominated by zircon, lack kyanite, sillimanite, andalusite, epidote and staurolite, and which are interpreted to have been derived from the Crocker and Rajang Groups of northern Borneo (Suggate 2011).

U–Pb dating studies of detrital zircons from the Tajau Sandstone Member indicate that the dominant age population is Jurassic and Early Cretaceous. Late Cretaceous, Permian–Triassic, Palaeozoic and Proterozoic zircons are present but do not form significant populations. Cenozoic (Paleocene to Eocene, 56 Ma to 41 Ma) zircons are present. The presence of unabraded Jurassic and Cretaceous zircons, apatite, detrital garnet, and the presence of rare metamorphic minerals such as kyanite and andalusite suggest that the Tajau Sandstone Member has an unusual metamorphic provenance. The main zircon age populations observed in the Sikuati Member are different to those of the Tajau Sandstone Member. The significant age groups observed are abraded Cretaceous, Permian–Triassic and Proterozoic (Neoproterozoic and Palaeoproterozoic) zircons and are broadly the same as those seen in the other Neogene sandstones in northern Borneo (Suggate 2011).

One potential source is the Palaeogene Crocker Group sandstones of northern Borneo which is characterized by typical continent-derived quartz-rich sediments with heavy minerals such as zircon, tourmaline and apatite. The Crocker Group sandstones were derived from the Schwaner Mountain granites and nearby Sunda Shelf and Malay–Thai Tin Belt granites (van Hattum 2005; van Hattum *et al.* 2013). The dominant zircon age populations are Cretaceous, Permian–Triassic and Palaeozoic. However, the Crocker Group Sandstones cannot be the only source for the Tajau Sandstone Member. Kyanite is unknown, and Jurassic zircons are largely absent in the Crocker Group sandstones. Palawan was suggested by van Hattum (2005) to be a possible source since kyanite is reported from high pressure metamorphic rocks interpreted to be related to subduction (Encarnación *et al.* 1995).

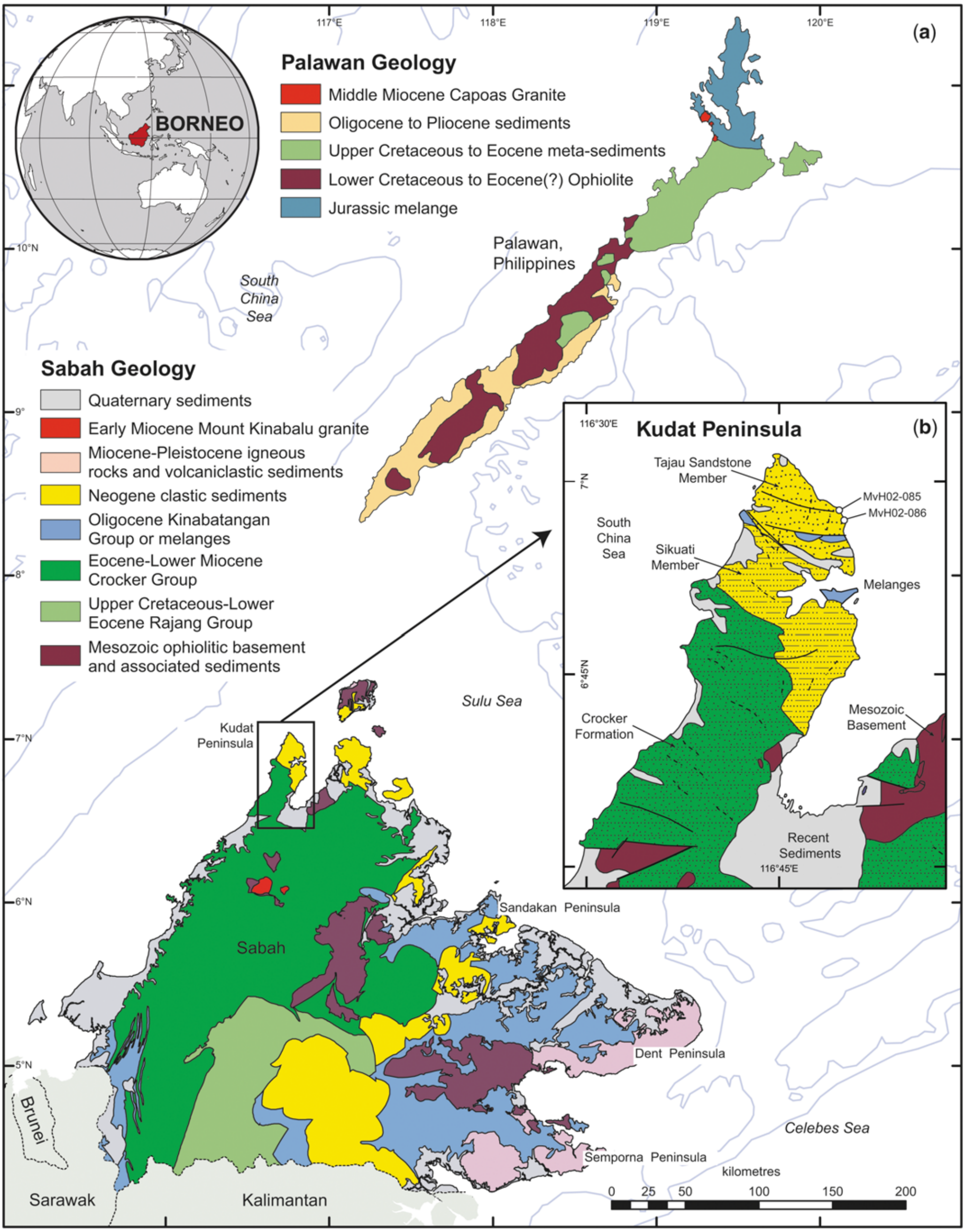

Fig. 6. (**a**) Geological map of northern Borneo and Palawan, Philippines, showing the main tectonostratigraphic provinces on land, modified from Lim & Heng (1985), Almasco *et al.* (2000), Mines & Geoscience Bureau, Philippines (2011) and Suggate (2011). (**b**) Inset shows geological map of the Kudat Peninsula, northern Sabah with locations of garnet-rich sandstone samples (van Hattum 2005) from the Tajau Sandstone Member, modified from Tongkul (1994) and Suggate (2011).

Detrital garnets

Detrital garnets are a significant component (*c.* 45%) of the heavy mineral assemblage from the Tajau Sandstone Member. Detrital garnets in this abundance are not known in other sandstones from Sabah. To help establish their provenance the garnet compositional database was used. The detrital garnets were analysed for major elements and their end-member compositions calculated. These compositions were plotted on ternary plots to identify possible protoliths using the methods described above, and compared with garnets from Palawan.

Sample locations and analytical techniques

A total of 43 detrital garnet grains hand picked from two samples (Fig. 6) from the Tajau Sandstone Member (MvH02-085 and MvH02-086) were embedded in epoxy resin and polished. Garnets from the Tajau Sandstone and a Kinabalu garnet peridotite were analysed for major elements (SiO_2, TiO_2, Al_2O_3, Cr_2O_3, Fe_2O_3, FeO, MnO, MgO, CaO and Na_2O) on a Jeol8100 Superprobe with an Oxford Instrument INCA micro-analytical system (EDS) at the Department of Earth and Planetary Sciences, Birkbeck College, University of London.

Detrital garnet compositions of the Neogene sandstones

Electron microprobe results and garnet end-member compositions for the detrital garnet grains analysed from samples MvH02-085 and MvH02-086 of the Tajau Sandstone Member are in Tables 4 and 5. Stages 1 and 2 were skipped as there were no garnets with rare oxides and high TiO_2. The garnets from the Tajau Sandstone Member are plotted on a ternary plot with provenance fields and fall into three sub-areas (Fig. 7).

Possible source areas of detrital garnets

One possible source for the Neogene sandstone detrital garnets are kyanite–garnet amphibolites exposed near the base of the pre-middle Eocene ophiolite described by Encarnación *et al.* (1995) on central Palawan, Philippines, north of the Kudat Peninsula. A second possible source is the garnet peridotites near Mount Kinabalu that form part of the Mesozoic crystalline basement of Sabah (Imai & Ozawa 1991).

Garnet end-member compositions for both possible sources were recalculated from major element analyses of eight garnets recorded by Encarnación *et al.* (1995), four garnets recorded by Imai & Ozawa (1991), and 14 new microprobe analyses from a garnet peridotite from Kinabalu made during this study. The garnet compositions are plotted on ternary plots with the provenance fields (Fig. 7a–d).

The garnet compositions in the kyanite–garnet amphibolites of central Palawan (Encarnación *et al.* 1995) are dominated by almandine–pyrope garnets (Alm49–59% and Prp12–36%). The majority of garnets plot within the field of amphibolites, granulites or sub-ophiolite soles, apart from one grain which plots within the blueschist field (Fig. 7a).

The average garnet compositions of the basement garnet peridotites of the Mount Kinabalu are dominated by a group of pyrope-rich (Prp60–76%) garnets with a small compositional range (Fig. 7b). This population is represented by Prp60–76%Alm13–26%Gro3–15%Sps0-1%. These garnets plot within the ultrabasic field (Fig. 7b).

Comparison between detrital garnets and possible sources

The garnets from the kyanite–garnet amphibolites on Palawan plot in an area that is typical of sub-ophiolite metabasites (Fig. 7c). If these were detrital garnets it would be possible to identify them as derived from amphibolites, granulites or sub-ophiolite soles; blueschists can be ruled out since several of the garnets are too enriched in pyrope.

The garnets from the basement peridotites of Mount Kinabalu area plot clearly within the peridotite field (Fig. 7b), demonstrating that the method correctly identifies them. There are no comparable detrital garnets from the Tajau Sandstone Member, indicating that they do not have a peridotite source. None of the detrital garnets from the Kudat Tajau Sandstone Member have a calc-silicate source.

On the ternary triangles the Kudat garnets fall into three groups (Fig. 7a). One group (Group A) is clearly derived from a granitic source (Fig. 7b). A second group (Group B) is almandine-rich. These garnets could be derived from amphibolites, granulites or sub-ophiolite soles (Fig. 7c), but not blueschists or granites. They plot close to the Palawan garnets. The third group (Group C) is almandine-rich and pyrope-poor. They could be derived from blueschists or amphibolites (Fig. 7d), but not granulites, sub-ophiolite soles, or granites.

Based on the ternary plots and the comparison to garnet compositions from Palawan and Kinabalu it is possible to rule out a Kinabalu source for any of the garnets, and imply a Palawan source for some of the garnets. The granitic garnets could come from Borneo or the Tin Belt, since granitic

Table 4. *Electron microprobe analyses of detrital garnets for sample MvH02-085, Tajau Sandstone Member, Kudat Formation*

Wt% oxide	1	2	3	4	5	6	7	8	9	10	11	12	13	14	15	16	17	18	19	20	21
SiO_2	37.57	37.41	38.47	38.33	37.13	36.87	37.67	37.39	37.46	37.98	37.22	37.24	36.30	36.65	37.13	37.35	37.08	36.87	36.87	35.52	35.78
Al_2O_3	19.65	20.51	20.90	20.86	20.65	20.96	21.52	21.18	20.96	20.91	20.60	20.73	19.46	20.55	20.60	21.36	20.83	20.98	19.86	18.76	19.08
TiO_2	0.12	0.14	0.06	0.09	0.02	0.00	0.02	0.02	0.05	0.04	0.02	0.03	0.00	0.07	0.09	0.07	0.11	0.01	0.01	0.17	0.16
Cr_2O_3	0.00	0.01	0.00	0.00	0.01	0.00	0.01	0.01	0.01	0.01	0.01	0.00	0.02	0.00	0.01	0.05	0.01	0.02	0.00	0.00	0.00
Fe_2O_3	0.27	0.46	0.00	0.01	0.13	0.33	0.00	0.03	0.70	0.17	0.20	0.00	0.47	0.57	0.65	0.25	0.63	0.79	1.02	1.47	1.25
FeO	23.55	23.87	27.17	27.02	34.76	34.45	30.34	30.36	28.37	28.85	34.92	34.93	32.35	32.94	29.28	29.82	27.77	24.74	24.27	19.31	19.66
MnO	6.21	6.26	2.68	2.72	2.94	2.85	6.47	6.38	2.44	2.49	1.66	1.66	4.39	4.48	2.17	2.08	1.64	5.92	6.04	20.82	20.81
MgO	1.29	1.28	5.19	5.32	2.85	2.84	3.71	3.61	4.68	4.57	3.16	3.26	2.99	3.04	3.90	3.79	0.69	1.37	1.34	0.76	0.75
CaO	10.03	9.58	5.10	5.16	1.21	1.28	1.03	1.04	4.38	4.63	1.68	1.64	1.00	0.74	4.72	4.64	10.68	8.41	8.73	0.57	0.59
Na_2O	0.01	0.02	0.02	0.01	0.01	0.01	0.03	0.03	0.01	0.00	0.03	0.00	0.00	0.01	0.00	0.02	0.02	0.03	0.03	0.03	0.02
Total	98.70	99.54	99.59	99.52	99.71	99.59	100.80	100.04	99.06	99.65	99.50	99.49	96.98	99.05	98.56	99.44	99.46	99.14	98.16	97.42	98.11
Formulae calculated on the basis of 24 oxygens. Fe_3 calculated for 16 cations																					
Si	6.092	6.014	6.066	6.049	6.018	5.978	5.989	5.998	5.980	6.028	6.024	6.022	6.056	5.981	5.990	5.965	5.973	5.957	6.027	6.016	6.014
Al	3.756	3.887	3.885	3.881	3.946	4.007	4.034	4.005	3.945	3.913	3.931	3.952	3.827	3.954	3.918	4.022	3.956	3.996	3.827	3.746	3.781
Ti	0.015	0.017	0.007	0.011	0.002	0.000	0.002	0.002	0.006	0.005	0.002	0.004	0.000	0.009	0.011	0.008	0.013	0.001	0.001	0.022	0.020
Cr	0.000	0.001	0.000	0.000	0.001	0.000	0.001	0.001	0.001	0.001	0.001	0.000	0.003	0.000	0.001	0.006	0.001	0.003	0.000	0.000	0.000
Fe_3	0.033	0.055	0.000	0.001	0.016	0.040	0.000	0.003	0.085	0.020	0.025	0.000	0.059	0.070	0.079	0.030	0.077	0.095	0.125	0.188	0.158
Fe_2	3.193	3.209	3.583	3.566	4.712	4.672	4.034	4.072	3.787	3.830	4.726	4.724	4.513	4.495	3.951	3.984	3.741	3.343	3.317	2.736	2.764
Mn	0.853	0.852	0.358	0.364	0.404	0.391	0.871	0.867	0.330	0.335	0.228	0.227	0.620	0.619	0.297	0.281	0.224	0.810	0.836	2.987	2.963
Mg	0.312	0.307	1.220	1.251	0.688	0.686	0.879	0.863	1.113	1.081	0.762	0.786	0.743	0.739	0.938	0.902	0.166	0.330	0.326	0.192	0.188
Ca	1.743	1.650	0.862	0.873	0.210	0.222	0.175	0.179	0.749	0.787	0.291	0.284	0.179	0.129	0.816	0.794	1.843	1.456	1.529	0.103	0.106
Na	0.003	0.006	0.006	0.003	0.003	0.003	0.009	0.009	0.003	0.000	0.009	0.000	0.000	0.003	0.000	0.006	0.006	0.009	0.010	0.010	0.007
End-members																					
Almandine	52.3	53.3	59.5	58.9	78.3	78.2	67.7	68.1	63.3	63.5	78.7	78.5	74.5	75.1	65.8	66.8	62.6	56.3	55.2	43.9	44.7
Andradite + Schorlomite	1.2	1.8	0.2	0.3	0.5	1.0	0.1	0.1	2.3	0.6	0.7	0.1	1.5	2.0	2.3	1.0	2.3	2.4	3.2	5.0	4.3
Grossulur	27.4	25.6	14.1	14.1	3.0	2.7	2.9	2.8	10.2	12.4	4.1	4.6	1.4	0.2	11.3	12.2	28.6	22.0	22.3	0.0	0.0
Pyrope	5.1	5.1	20.3	20.7	11.4	11.5	14.7	14.4	18.6	17.9	12.7	13.0	12.3	12.4	15.6	15.1	2.8	5.6	5.4	3.1	3.0
Spessartine	14.0	14.2	5.9	6.0	6.7	6.6	14.6	14.5	5.5	5.5	3.8	3.8	10.2	10.4	4.9	4.7	3.7	13.6	13.9	48.0	47.9
Uvarovite	0.0	0.0	0.0	0.0	0.0	0.0	0.0	0.0	0.0	0.0	0.0	0.0	0.1	0.0	0.0	0.2	0.0	0.1	0.0	0.0	0.0

Table 5. *Electron microprobe analyses of detrital garnets for sample MvH02-086, Tajau Sandstone Member, Kudat Formation*

Wt% oxide	1	2	3	4	5	6	7	8	9	10	11	12	13	14	15	16	17	18	19	20	21	22
SiO_2	38.81	38.46	38.54	96.72	37.68	37.79	37.76	37.75	38.08	38.21	34.01	34.30	37.96	37.49	32.96	34.29	38.65	38.99	37.31	36.76	37.93	38.34
Al_2O_3	21.65	21.11	21.28	0.02	21.13	21.28	21.19	20.92	21.38	21.51	0.01	0.00	20.81	20.81	0.02	0.00	21.84	21.74	20.18	20.28	21.05	21.48
TiO_2	0.05	0.01	0.06	0.02	0.02	0.00	0.02	0.04	0.00	0.01	0.03	0.05	0.00	0.01	0.00	0.00	0.03	0.03	0.09	0.08	0.10	0.10
Cr_2O_3	0.01	0.00	0.00	0.00	0.01	0.02	0.00	0.01	0.00	0.03	0.00	0.00	0.02	0.01	0.00	0.00	0.01	0.02	0.00	0.01	0.00	0.02
FeO	29.17	28.89	29.02	0.65	33.13	33.06	32.79	32.71	34.18	34.97	0.00	0.00	34.11	34.11	0.02	0.00	0.00	0.00	0.00	0.11	0.00	0.00
MnO	3.11	3.10	3.14	0.07	4.56	4.67	5.18	5.31	2.70	2.45	0.01	0.00	2.32	2.31	0.00	0.00	28.56	28.48	20.18	20.02	26.00	26.68
MgO	4.96	5.06	4.85	0.00	2.24	2.22	2.42	2.39	2.99	3.00	0.00	0.00	3.15	3.16	0.01	0.01	2.74	2.63	18.80	18.74	4.83	3.15
CaO	3.09	3.65	3.53	0.30	1.35	1.24	0.95	1.03	1.18	1.07	0.00	0.03	1.43	1.43	0.09	0.02	4.50	4.56	1.25	1.26	0.77	0.80
Na_2O	0.00	0.01	0.00	0.02	0.02	0.04	0.04	0.04	0.03	0.02	0.02	0.02	0.02	0.01	0.06	0.01	4.60	4.72	1.75	1.93	9.54	10.31
K_2O	0.01	0.00	0.00	0.01	0.00	0.00	0.00	0.00	0.01	0.00	0.01	0.00	0.00	0.00	0.04	0.01	0.01	0.03	0.06	0.06	0.01	0.02
Total	100.86	100.29	100.42	97.81	100.14	100.32	100.35	100.20	100.55	101.27	101.27	101.27	99.82	99.34	33.20	33.20	100.94	101.20	99.63	99.26	100.24	100.90
Formulae calculated on the basis of 24 oxygens. Fe_3 calculated for 16 cations																						
Si	6.059	6.052	6.056	11.937	6.063	6.066	6.062	6.075	6.069	6.054	6.054	6.054	6.095	6.057	11.955	11.955	6.030	6.060	6.090	6.032	6.050	6.051
Al	3.985	3.916	3.942	0.003	4.009	4.027	4.011	3.969	4.017	4.018	4.018	4.018	3.939	3.964	0.009	0.009	4.017	3.983	3.883	3.923	3.959	3.996
Ti	0.006	0.001	0.007	0.002	0.002	0.000	0.002	0.005	0.000	0.001	0.001	0.001	0.000	0.001	0.000	0.000	0.004	0.004	0.011	0.010	0.012	0.012
Cr	0.001	0.000	0.000	0.000	0.001	0.003	0.000	0.001	0.000	0.004	0.004	0.004	0.003	0.001	0.000	0.000	0.001	0.002	0.000	0.001	0.000	0.002
Fe_2	3.809	3.802	3.814	0.067	4.459	4.438	4.402	4.403	4.556	4.634	4.634	4.634	4.580	4.609	0.006	0.006	0.000	0.000	0.000	0.014	0.000	0.000
Mn	0.411	0.413	0.418	0.007	0.622	0.635	0.704	0.724	0.364	0.329	0.329	0.329	0.316	0.316	0.000	0.000	3.727	3.702	2.755	2.747	3.469	3.521
Mg	1.154	1.187	1.136	0.000	0.537	0.531	0.579	0.573	0.710	0.708	0.708	0.708	0.754	0.761	0.005	0.005	0.362	0.346	2.599	2.605	0.653	0.421
Ca	0.517	0.615	0.594	0.040	0.233	0.213	0.163	0.178	0.201	0.182	0.182	0.182	0.246	0.248	0.035	0.035	1.046	1.056	0.304	0.308	0.183	0.188
Na	0.000	0.003	0.000	0.005	0.006	0.012	0.012	0.012	0.009	0.006	0.006	0.006	0.006	0.003	0.042	0.042	0.769	0.786	0.306	0.339	1.631	1.743
K	0.002	0.000	0.000	0.002	0.000	0.000	0.000	0.000	0.002	0.000	0.000	0.000	0.000	0.000	0.019	0.019	0.003	0.009	0.019	0.019	0.003	0.006
End-members																						
Almandine	64.7	63.2	64.0	58.8	76.2	76.3	75.3	74.9	78.1	79.2	79.2	79.2	77.7	77.7	13.1	13.1	63.1	62.8	46.2	45.8	58.4	59.9
Andradite + Schorlomite	0.1	0.0	0.2	2.4	0.1	0.0	0.1	0.1	0.0	0.0	0.0	0.0	0.0	0.0	0.0	0.0	0.1	0.1	0.3	0.6	0.3	0.3
Grossulur	8.6	10.2	9.8	32.3	3.9	3.6	2.7	2.9	3.5	3.0	3.0	3.0	4.1	4.1	75.3	75.3	12.9	13.2	4.9	5.0	27.2	29.3
Pyrope	19.6	19.7	19.1	0.0	9.2	9.1	9.9	9.8	12.2	12.1	12.1	12.1	12.8	12.8	11.6	11.6	17.7	17.9	5.1	5.1	3.1	3.2
Spessartine	7.0	6.9	7.0	6.4	10.6	10.9	12.0	12.3	6.2	5.6	5.6	5.6	5.4	5.3	0.0	0.0	6.1	5.9	43.6	43.4	11.0	7.2
Uvarovite	0.0	0.0	0.0	0.0	0.0	0.1	0.0	0.0	0.0	0.1	0.1	0.1	0.1	0.0	0.0	0.0	0.0	0.1	0.0	0.0	0.0	0.1

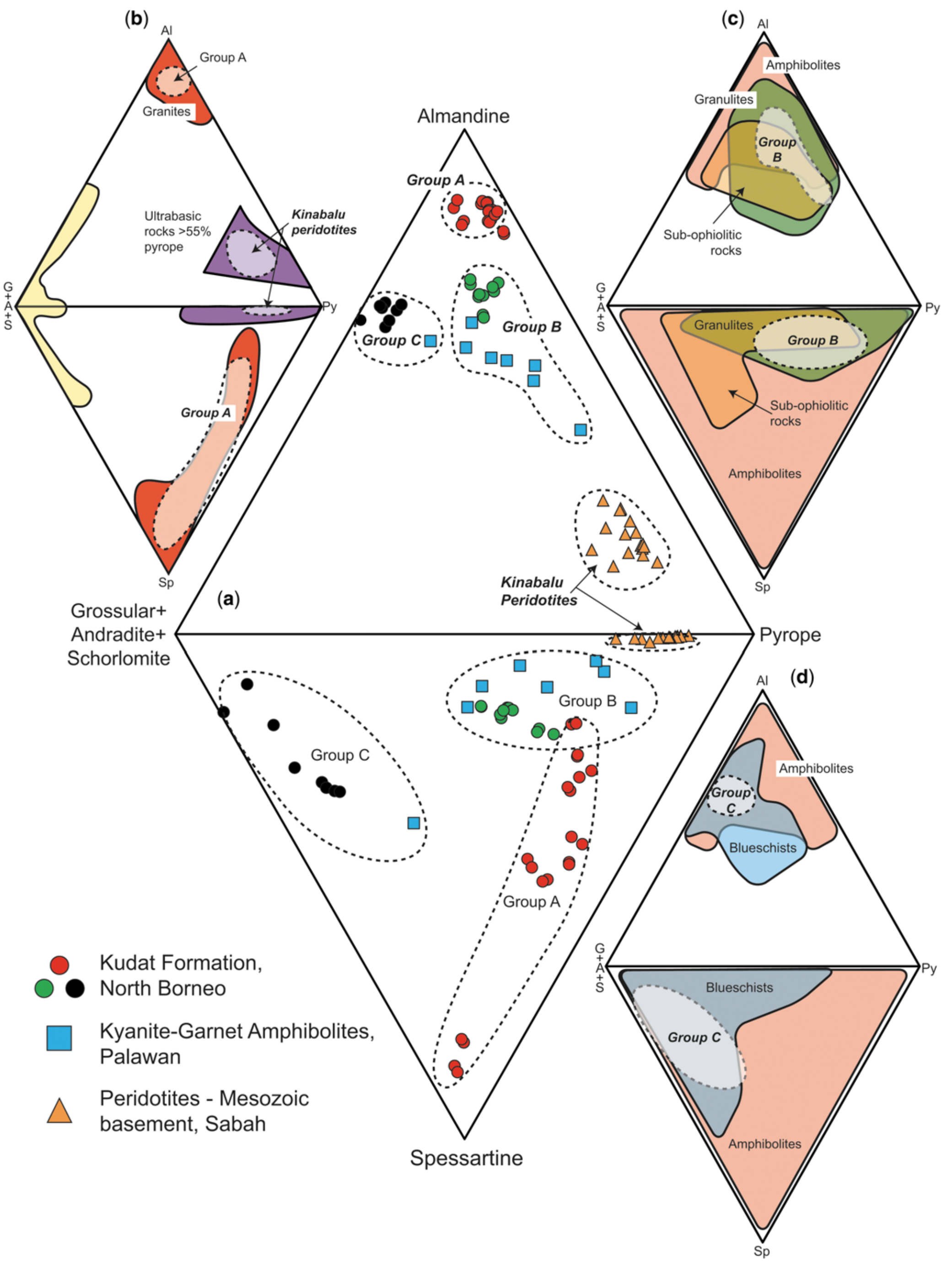

Fig. 7. Ternary plots using end-members grossular + andradite + schorlomite, almandine, pyrope and spessartine. (**a**) Individual grain compositions and provenance groups for detrital garnets from the Tajau Sandstone Member, Kudat Formation, Sabah compared to garnets from kyanite-garnet amphibolites on Palawan (Encarnación *et al.* 1995), and garnets from peridotites of the Sabah basement (Imai & Ozawa 1991; this study). (**b**–**d**) Ternary plots showing sub-areas characteristic of garnets with different protoliths, from Figure 4, with inferred protoliths of Kudat detrital garnets.

rocks are known to be the source of Crocker Group sediments which have been recycled into other Neogene sandstones. However, garnets are not abundant in the Crocker Group heavy mineral assemblages (van Hattum 2005; van Hattum *et al.* 2013). We suggest it is likely that the granitic garnets are derived from either Cretaceous and Jurassic granites that rifted away from the South China margin during the opening of the South China Sea in the Early Oligocene (Taylor & Hayes 1983; Hall 2002; Franke *et al.* 2011) and are now part of the North Palawan Continental Terrane (e.g. Encarnación *et al.* 1995; Encarnación & Mukasa 1997; Knittel *et al.* 2010), or they were derived from Middle Eocene South China Sea rift-related granites that are exposed in Central Palawan.

In addition to the unusual abundance of garnets, the presence of other metamorphic minerals such as kyanite supports a Palawan source. Kyanite is not known from Palaeogene Crocker Group sediments on Borneo, but is known from kyanite–garnet amphibolites in central Palawan (Encarnación *et al.* 1995). Thus a Palawan source for the Kudat detrital garnets seems more likely. The source of the third group of garnets is not known. Their compositions indicate a blueschist facies or amphibolite facies origin. Rare blueschists have been reported from Sabah (Leong 1978), but little is known of them. Subduction-related rocks are described from Palawan (Encarnación *et al.* 1995), so blueschists could be expected there. Amphibolite facies rocks are known from the Schwaner region of Kalimantan. Nothing is currently known of garnet compositions from any of these areas.

Early Miocene palaeogeography of Northern Borneo

During the Early Miocene two river systems deposited sediment in offshore northern Borneo in a shallow-marine setting (Tajau Sandstone Member). Rivers flowed northwards draining the Crocker Mountains contributing recycled quartz-rich material from the Crocker Group sandstones, originally derived from granitic rocks in the Schwaner Mountain of SE Kalimantan, nearby Sunda Shelf and Malay–Thai Tin Belt (van Hattum *et al.* 2006, 2013). At the same time, southward-flowing rivers drained the granitic and metamorphic rocks on Palawan, depositing sediments containing garnets derived from granites, amphibolites, granulites and sub-ophiolite soles.

Conclusions

There have been many studies that have related garnet compositions to sources. This study confirms that detrital garnet compositions are very useful in provenance studies, and can be used to determine protoliths. However, many common garnet compositions are not completely diagnostic of protoliths, although if the garnets have local sources, quite accurate matches can be made. This study shows that compositional data from a large global database can be reliably used to infer protoliths and provenance, which is particularly useful for regions where the sources are unknown, have been removed by erosion, or there are no compositional data from local garnet-bearing rocks. By using a specific sequence of steps and ternary plots, garnets can be matched to sources.

Testing the method with sandstones from northern Borneo shows that the garnet-rich heavy mineral assemblages of the Kudat Formation Tajau Sandstone Member probably came from granitic, blueschist and amphibolite sources. Such rocks are known from Palawan, and some garnet compositions match well. The discovery of the unusual heavy mineral assemblages of the Tajau Sandstone Member was unexpected and confirms the value of garnet as a provenance indicator in certain circumstances.

The project was funded by the SE Asia Research Group at Royal Holloway University of London, supported by an oil company consortium. We thank the Economic Planning Unit Malaysia for permission to conduct field work and Allagu Balaguru for field support. A. Carter and A. Beard at University College London and Birkbeck College, University of London are thanked for their help with analytical work. L. Davies and P. Hall are thanked for help in compiling the garnet compositional data from the published literature. We are grateful to J. Wakabayashi and A. Okay for information on high pressure garnets. We thank E. Garzanti for permission to use the Alpine garnet data and for invaluable discussion of garnet provenance.

References

Almasco, J. N., Rodolfo, K., Fuller, M. & Frost, G. 2000. Paleomagnetism of Palawan, Philippines. *Journal of Asian Earth Sciences*, **18**, 369–389.

Andò, S., Morton, A. C. & Garzanti, E. 2013. Metamorphic grade of source rocks revealed by chemical fingerprints of detrital amphibole and garnet. *In*: Scott, R. A., Smyth, H. R., Morton, A. C. & Richardson, N. (eds) *Sediment Provenance Studies in Hydrocarbon Exploration and Production*. Geological Society, London, Special Publications, 386. First published online June 20, 2013, http://dx.doi.org/10.1144/SP386.5

Aubrecht, R., Méres, Š., Sýkora, M. & Mikuš, T. 2009. Provenance of the detrital garnets and spinels from the Albian sediments of the Czorsztyn Unit (Pieniny Klippen Belt, Western Carpathians, Slovakia). *Geologica Carpathica*, **60**, 463–483.

BouDagher-Fadel, M. 2008. *Evolution and Geological Significance of Larger Benthic Foraminifera.* Developments in Palaeontology and Stratigraphy, Elsevier, Amsterdam, **21**.

Clement, J. F. & Keij, J. 1958. Geology of the Kudat Peninsula, North Borneo (Compilation). GR783, unpublished reports of the Royal Dutch Shell Group of Companies in British Borneo.

Coleman, R. G., Lee, D. E., Beatty, L. B. & Brannock, W. W. 1965. Eclogites and eclogites: their differences and similarities. *Geological Society of America Bulletin*, **76**, 483–508.

Copjakova, R., Sulovsky, P. & Paterson, B. A. 2005. Major and trace elements in pyrope-almandine garnets as sediment provenance indicators of the Lower Carboniferous Culm sediments, Drahany Uplands, Bohemian Massif. *Lithos*, **82**, 51–70.

Deer, W. A., Howie, R. A. & Zussman, J. 1962. *Rock-Forming Minerals, Volume 1 (Ortho and Ring Silicates)*. Longmans, London.

Deer, W. A., Howie, R. A. & Zussman, J. 1966. *An Introduction to the Rock Forming Minerals.* Longmans, London.

Deer, W. A., Howie, R. A. & Zussman, J. (eds) 1997. *Rock-Forming Minerals, Volume 1A, Orthosilicates*. 2nd edn. Geological Society, London.

Encarnación, J. & Mukasa, S. B. 1997. Age and geochemistry of an 'anorogenic' crustal melt and implications for I-type granite petrogenesis. *Lithos*, **42**, 1–13.

Encarnación, J. P., Essene, E. J., Mukasa, S. B. & Hall, C. H. 1995. High pressure and temperature subophiolitic kyanite-garnet amphibolites generated during initiation of mid Tertiary subduction, Palawan, Philippines. *Journal of Petrology*, **36**, 1481–1503.

Evans, B. W. & Trommsdorff, V. 1978. Petrogenesis of garnet lherzolite, Cima di Gagnone, Lepontine Alps. *Earth and Planetary Science Letters*, **40**, 333–348.

Franke, D., Barckhausen, U. *et al.* 2011. The continent–ocean transition at the southeastern margin of the South China Sea. *Marine and Petroleum Geology*, **28**, 1187–1204.

Galuskina, I. O., Galuskin, E. V., Dzierzanowski, P., Armbruster, T. & Kozanecki, M. 2005. A natural scandian garnet. *American Mineralogist*, **90**, 1688–1692.

Hall, R. 2002. Cenozoic geological and plate tectonic evolution of SE Asia and the SW Pacific: computer-based reconstructions, model and animations. *Journal of Asian Earth Sciences*, **20**, 353–434.

Hallsworth, C. R. & Chisholm, J. I. 2008. Provenance of late Carboniferous sandstones in the Pennine Basin (UK) from combined heavy mineral, garnet geochemistry and palaeocurrent studies. *Sedimentary Geology*, **203**, 196–212.

Haughton, P. D. W. & Farrow, C. M. 1989. Compositional variation in Lower Old Red Sandstone detrital garnets from the Midland Valley of Scotland and the Anglo-Welsh Basin. *Geological Magazine*, **126**, 373–396.

Hutchison, A. R. & Oliver, G. J. H. 1998. Garnet provenance studies, juxtaposition of Laurentian marginal terranes and timing of the Grampian orogeny in Scotland. *Journal of the Geological Society, London*, **155**, 541–550.

Imai, A. & Ozawa, K. 1991. Tectonic implications of the hydrated garnet peridotites near Mt Kinabalu, Sabah, East Malaysia. *Journal of Southeast Asian Earth Sciences*, **6**, 431–446.

Kahoui, M., Kaminsky, F. V., Griffin, W. L., Belousova, E., Mahdjoub, Y. & Chabane, M. 2012. Detrital pyrope garnets from the El Kseibat area, Algeria: a glimpse into the lithospheric mantle beneath the north-eastern edge of the West African Craton. *Journal of African Earth Sciences*, **63**, 1–11.

Knittel, U., Hung, C.-H., Yang, T. F. & Iizuka, Y. 2010. Permian arc magmatism in Mindoro, the Philippines: an early Indosinian event in the Palawan Continental Terrane. *Tectonophysics*, **493**, 113–117.

Knowles, C. R. 1987. A BASIC program to recast garnet end-members. *Computers & Geosciences*, **13**, 655–658.

Leong, K. M. 1978. The 'Sabah Blueschist Belt' – a preliminary note. *Warta Geologi, Geological Society of Malaysia Newsletter*, **4**, 45–51.

Lim, P. S. & Heng, Y. E. 1985. Geological Map of Sabah 1:500 000. *In*: *Geological Survey of Malaysia*, Ministry of Lands and Mines, Malaysia.

Locock, A. J. 2008. An Excel spreadsheet to recast analyses of garnet into end-member components, and a synopsis of the crystal chemistry of natural silicate garnets. *Computers & Geosciences*, **34**, 1769–1780.

Mange, M. A. & Morton, A. C. 2007. Geochemistry of heavy minerals. *In*: Mange, M. A. & Wright, D. T. (eds) *Heavy Minerals in Use*. Developments in Sedimentology, Elsevier, Amsterdam, **58**, 345–391.

Martínek, K. & Štolfová, K. 2009. Provenance study of Permian non-marine sandstones and conglomerates of the Krkonoše Piedmont Basin (Czech Republic): exotic marine limestone pebbles, heavy minerals and garnet composition. *Bulletin of Geosciences*, **84**, 555–568.

Méres, Š., Aubrecht, R., Gradziński, M. & Sýkora, M. 2012. High (ultrahigh) pressure metamorphic terrane rocks as the source of the detrital garnets from the Middle Jurassic sands and sandstones of the Cracow Region (Cracow-Wieluń Upland, Poland). *Acta Geologica Polonica*, **2**, 231–246.

MINES AND GEOSCIENCE BUREAU, PHILIPPINES 2011. *Geological map of Northern Palawan*. Mines and Geosciences Bureau, Quezon City, Phillipines.

Morton, A. C. 1985. A new approach to provenance studies–electron-microprobe analysis of detrital garnets from Middle Jurassic sandstones of the northern North Sea. *Sedimentology*, **32**, 553–566.

Morton, A., Hallsworth, C. & Chalton, B. 2004. Garnet compositions in Scottish and Norwegian basement terrains: a framework for interpretation of North Sea sandstone provenance. *Marine and Petroleum Geology*, **21**, 393–410.

Muhling, J. R. & Griffin, B. J. 1991. On recasting garnet analyses into end-member molecules–revisited short note. *Computers & Geosciences*, **17**, 161–170.

Nimis, P. & Trommsdorff, V. 2001. Revised thermobarometry of Alpe Arami and other garnet peridotites from the Central Alps. *Journal of Petrology*, **42**, 103–115.

Oliver, G. J. H. 2001. Reconstruction of the Grampian episode in Scotland: its place in the Caledonian Orogeny. *Tectonophysics*, **332**, 23–49.

Rickwood, P. C. 1968. On recasting analyses of garnet into end-member molecules. *Contributions to Mineralogy and Petrology*, **18**, 175–198.

Sabeen, H. M., Ramanujam, N. & Morton, A. C. 2002. The provenance of garnet: constraints provided by studies of coastal sediments from southern India. *Sedimentary Geology*, **152**, 279–287.

Stephens, E. A. 1956. The geology and mineral resources of the Kota Belud and Kudat area, North Borneo. *Malaysia Geological Survey Borneo Region, Memoir*, **5**, 137.

Suggate, S. 2011. *Provenance of Neogene sandstones of Sabah, northern Borneo.* PhD thesis, Royal Holloway University of London.

Takeuchi, M. 1994. Changes in garnet chemistry show a progressive denudation of the source areas for Permian-Jurassic sandstones, Southern Kitakami Terrane, Japan. *Sedimentary Geology*, **93**, 85–105.

Takeuchi, M., Kawai, M. & Matsuzawa, N. 2008. Detrital garnet and chromian spinel chemistry of Permian clastics in the Renge area, central Japan: implications for the paleogeography of the East Asian continental margin. *Sedimentary Geology*, **212**, 25–39.

Taylor, B. & Hayes, D. E. 1983. Origin and history of the South China Sea Basin. *In*: Hayes, D. E. (ed.) *The Tectonic and Geologic Evolution of Southeast Asian Seas and Islands, Part 2. 27*, American Geophysical Union, Washington, DC, Geophysical Monographs Series, 23–56.

Tebbens, L. A., Kroonenberg, S. B. & van den Berg, M. W. 1995. Compositional variation of detrital garnets in Quaternary Rhine, Meuse and Baltic River sediments in the Netherlands. *Geologie en Mijnbouw*, **74**, 213–224.

Tongkul, F. 1994. The geology of northern Sabah, Malaysia – its relationship to the opening of the South China Sea Basin. *Tectonophysics*, **235**, 131–147.

van Hattum, M. 2005. *Provenance of Cenozoic Sedimentary Rocks of Northern Borneo.* PhD thesis, University of London.

van Hattum, M., Hall, R., Pickard, A. L. & Nichols, G. J. 2006. Southeast Asian sediments not from Asia: provenance and geochronology of north Borneo sandstones. *Geology*, **34**, 589–592.

van Hattum, M., Hall, R., Pickard, A. L. & Nichols, G. J. 2013. Provenance and geochronology of Cenozoic sandstones of northern Borneo. *Journal of Asian Earth Sciences*, in press.

Win, K. S., Takeuchi, M., Iwakiri, S. & Tokiwa, T. 2007. Provenance of detrital garnets from the Yukawa Formation, Yanase district, Shimanto belt, Kii Peninsula, Southwest Japan. *Journal of the Geological Society of Japan*, **113**, 133–145.